

Supporting Information for

Self-Degradable Photosensitizer Exhibiting Bacterial Agglutination and Membrane Insertion toward Safe Photodynamic Ablation

Chengcheng Zhou,^{*a} Yimei Li,^a Yihui Shen,^a Ze Lv,^b Jianguo Feng,^b Meijuan Jiang,^c Jian Du,^d and Weijiang Guan^{*e}

^aSchool of Chemistry and Chemical Engineering, Yangzhou University, Yangzhou 225002, China

^bCollege of Plant Protection, Yangzhou University, Yangzhou 225009, China

^cDepartment of Chemistry, The Hong Kong University of Science and Technology, Clear Water Bay, Kowloon, Hong Kong, China

^dDepartment of Urology, The First Affiliated Hospital of Shandong First Medical University, NO. 16766, Jingshi Road, Jinan 250000, China

^eState Key Laboratory of Chemical Resource Engineering, Beijing University of Chemical Technology, Beijing 100029, China

*Corresponding authors: zhoucc@yzu.edu.cn; wjguan@mail.buct.edu.cn

Materials

(6-(4-(7-(diethylamino)-2-oxo-2H-chromen-3-yl)phenyl)-3,4-diphenyl-2-propylisoquinolin-2-ium) IQ-Cm and *N*-dodecyl- β -D-galactosamine (DGal) were synthesized referring to the previous report¹. Commercial singlet oxygen (¹O₂) indicator 9,10-anthracenediyl-bis(methylene) dimalonic acid (ABDA), hydroxyl radical ([•]OH) probe hydroxyphenyl fluorescein (HPF), reactive oxygen species (ROS) probe 2',7'-Dichlorofluoresceindiacetate (DCFH-DA), and phosphate buffered saline (1 × PBS, pH 7.4) were purchased from Sigma-Aldrich, ThermoFisher, Energy Chemical and WISENT corporation. *Pseudomonas aeruginosa* (*P. aeruginosa*, CMCC(B) 10104) was obtained from Beijing Microbiological Culture Collection Center.

Experimental methods

Characterization of DGal. The chemical structure of DGal was identified by ¹H magnetic resonance (¹H NMR, Fig. S23) and high-resolution mass spectrometry (HRMS, Fig. 24). ¹H NMR (400 MHz, DMSO-*d*₆) δ 4.2-4.7 (m, 4H), 3.7-3.4 (m, 5H) 3.29 (t, 2H), 3.21 (t, 1H), 2.79 (m, 1H), 2.49 (m, 1H), 2.15 (m, 1H), 1.41 (t, 2H), 1.28 (m, 18H), 0.89 (t, 3H). HRMS (MALDI-TOF) (m/z): [M+H]⁺ calcd for C₁₈H₃₈NO₅⁺, 348.2744, found 348.2747; [M+Na]⁺ calcd for C₁₈H₃₇NO₅Na⁺, 370.2564 found, 370.2569.

Preparation of IQ-Cm/DGal aggregates. 5 mM of IQ-Cm and 10 mM of DGal stock solution in DMSO were prepared and diluted with PBS to the required concentration for the experiment. The concentration of IQ-Cm was fixed at 20 μ M and different

amount of DGal was added to prepare different molar ratios of IQ-Cm/DGal aggregates.

Preparation of bacteria suspension. A single colony of *P. aeruginosa* was introduced into 10 mL of liquid LB culture medium, followed by incubation under shaking of 180 rpm at 37 °C for approximately 8~10 h. Subsequently, the *P. aeruginosa* were harvested by centrifugation (7100 rpm, 2 min), and washed twice with PBS. The harvested *P. aeruginosa* were resuspended in PBS, and then the optical density was adjusted to 1.0 at 600 nm ($OD_{600} = 1.0$).

Transmission electron microscopy (TEM). The morphology of IQ-Cm/DGal aggregates before and after 30 min of light irradiation (60 mW/cm², denoted as L30) was observed by TEM. 10 μL of IQ-Cm/DGal sample was dropped onto a 230 mesh copper grid, adsorbed for about 1 min, and then excess sample was removed with filter paper. Then, negative staining was performed with 10 μL of phosphotungstic acid solution for about 30 s, followed by removal of excess staining solution by filter paper. The samples were dried naturally and observed on a transmission electron microscope (HT7800, Hitachi, Japan).

Dynamic light scattering (DLS). The size distribution of IQ-Cm/DGal aggregates in PBS solution before and after L30, as well as the size change of *P. aeruginosa* ($OD_{600} = 1.0$) after incubated with IQ-Cm/DGal aggregates were measured on a Nano ZS (ZEN3690, Malvern) at a scattering angle of 173° at 25 °C.

Zeta potential measurements. The surface potential of IQ-Cm/DGal aggregates in PBS solution before and after L30, as well as *P. aeruginosa* ($OD_{600} = 1.0$) before and after incubated with IQ-Cm/DGal aggregates were measured on a Nano ZS at a

scattering angle of 173° at 25 °C.

HRMS of IQ-Cm. The products of IQ-Cm molecules before and after L30 were characterized in positive ion mode on a Mass Spectrometer (Bruker Maxis, Germany).

ROS detection. ROS generation ability of IQ-Cm/DGal aggregates before and after L30 was assessed using the commercial indicator ABDA for type II ROS ($^1\text{O}_2$) and HPF probe for type I ROS ($\cdot\text{OH}$). For $^1\text{O}_2$ detection: 10 μL of ABDA solution (10 mM) was added to 2 mL of IQ-Cm/DGal solutions. The absorption spectra of ABDA were then collected under white light irradiation (20 mW/cm^2) for different time using a spectrophotometer (UV-6100, Mapada, China). For $\cdot\text{OH}$ detection: 5 μM of HPF probe was added to into IQ-Cm/DGal solutions. The fluorescence emission spectra of HPF from 500 nm to 580 nm were recorded with an excitation wavelength of 490 nm under white light exposure (20 mW/cm^2) for different time on a fluorescence spectrometer (F7000, Hitachi, Japan).

In situ detection of ROS: *In situ* ROS generation in *P. aeruginosa* clusters induced by IQ-Cm/DGal aggregates at molar ratios of 1:0 and 1:0.8 under white light irradiation was detected using DCFH-DA. *P. aeruginosa* suspension (100 μL , $\text{OD}_{600} = 1.0$) was incubated with DCFH-DA (50 μM) in final volume of 500 μL PBS solution for 20 min, centrifuged (7100 rpm, 2 min) and then washed with PBS twice to remove the unbound DCFH-DA. Subsequently, the as-prepared *P. aeruginosa* were incubated with 500 μL of IQ-Cm/DGal aggregates (20 μM) for 10 min in darkness, and then irradiated under white light for 40 s. After centrifugation (7100 rpm, 2 min) to remove the supernatant, the *P. aeruginosa* was resuspended in 10 μL of PBS solution. 2 μL of the suspension

was placed onto a slide, and then imaged using a confocal laser microscope (LSM 880NLO, Carl Zeiss, Germany) with a $\times 100$ oil lens. Imaging conditions: Ex: 488 nm and Em: 501–627 nm. Control experiments included *P. aeruginosa* treated with IQ–Cm/DGal aggregates and DCFH-DA without light irradiation, only IQ–Cm/DGal aggregates under light irradiation, or only DCFH-DA under light irradiation, following the same procedures above.

Flow cytometric analysis of ROS generation: *P. aeruginosa* were treated with IQ–Cm/DGal aggregates and DCFH-DA following the conditions for *in situ* detection of ROS above. The fluorescence signals of as-prepared *P. aeruginosa* were collected in the FITC channel using a flow cytometer (LSRFortessa, BD, USA).

Oxidative degradation property. Vitamin C (VC) was used to verify that the degradation of IQ-Cm resulted from the ROS generated by IQ-Cm/DGal aggregates under white light irradiation. Specifically, 800 μM of VC was added to IQ-Cm/DGal aggregates solution, then the fluorescence spectra were recorded under white light irradiation ($60 \text{ mW}/\text{cm}^2$) for different time on a fluorescence spectrometer (F7000, Hitachi, Japan). The fluorescence spectra of IQ-Cm/DGal aggregates without the addition of VC under different time of white light irradiation were collected as control groups.

CLSM imaging of bacteria. *P. aeruginosa* suspension (100 μL , $\text{OD}_{600} = 1.0$) was incubated by 20 μM of IQ-Cm/DGal aggregates at different molar ratios in final volume of 500 μL PBS solution for different time at 37 $^{\circ}\text{C}$. The supernatant was then removed by centrifugation (7100 rpm, 2 min) and the harvested *P. aeruginosa* were resuspended

in 10 μL of PBS. 2 μL of as-prepared *P. aeruginosa* suspension was dropped onto a glass slide, and then imaged under a confocal laser microscope (LSM 880NLO, Carl Zeiss, Germany) with a $\times 100$ oil lens. Imaging conditions: Ex: 405 nm and Em: 420-570 nm.

Evaluation of antibacterial activity. The killing efficiency of IQ-Cm/DGal aggregates against *P. aeruginosa* was evaluated by surface plating method according to the previous report². To assess the killing efficiency of IQ-Cm/DGal aggregates under light irradiation: *P. aeruginosa* (100 μL , $\text{OD}_{600} = 1.0$) in final volume of 500 μL PBS solution was treated by 20 μM of IQ-Cm/DGal aggregates at different molar ratios in darkness for 10 min at 37 $^{\circ}\text{C}$, and then irradiated under white light (60 mW/cm^2) for 30 min. Following a 10^4 -fold dilution with PBS, 100 μL of the diluted bacterial solution was evenly spread on LB solid medium and cultured for 10-12 h at 37 $^{\circ}\text{C}$. For the assessment of killing efficiency of IQ-Cm/DGal aggregates under darkness, a similar procedure was performed, replacing the light irradiation with a 30 min dark incubation. For the killing efficiency of IQ-Cm/DGal aggregates after L30: IQ-Cm/DGal aggregates were exposed to white light (60 mW/cm^2) for 30 min before being utilized in antibacterial activity experiments as described above. The killing efficiency of IQ-Cm/DGal aggregates at different molar ratios was calculated: killing efficiency (%) = $(A-B)/A \times 100\%$, where A and B represent the average *P. aeruginosa* colonies without and with IQ-Cm/DGal aggregates, respectively.

Scanning electron microscopy (SEM). The morphology change of *P. aeruginosa* before and after treated with IC-Cm/DGal aggregates was observed by SEM

(Zeiss_Supra55, Germany). *P. aeruginosa* was treated with IQ-Cm/DGal aggregates following the procedures described in the section "Evaluation of antibacterial activity" above. Subsequently, the bacterial suspension was treated following the procedures described in the reference before SEM observations².

Cytotoxicity. The cytotoxicity of IQ-Cm/DGal aggregates before and after L30 was evaluated using the Cell Counting Kit-8 (CCK-8). Specifically, 100 μ L of Lo2 cells (1×10^6 cells/mL) were seeded into 96-well plates and cultured until adherent. After removing the DMEM medium, the fresh DMEM medium with IQ-Cm/DGal aggregates (or IQ-Cm/DGal aggregates after L30) was added, and then incubated for 30 min. After removing the medium containing the samples, 100 μ L of fresh media was added and the cells were further incubated for 24 h at 37 °C. After removing the medium, 100 μ L of fresh medium containing 10 μ L of CCK-8 were added in each well and then cultured for 3 h. The absorbance of each well at 450 nm was measured using a microplate reader (SPARK, Tecan, Switzerland).

Supplementary figures

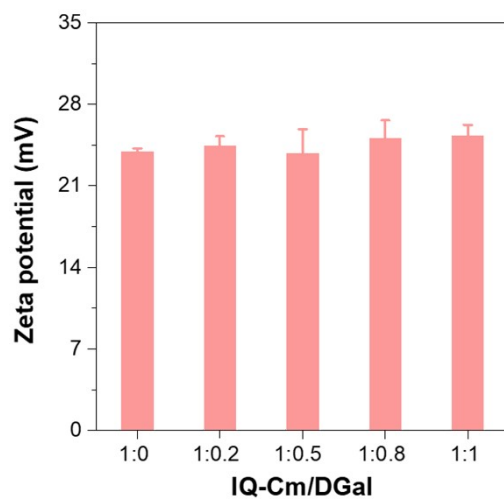


Fig. S1 Zeta potential results of IQ-Cm/DGal aggregates at different molar ratios. [IQ-Cm] = 20 μ M.

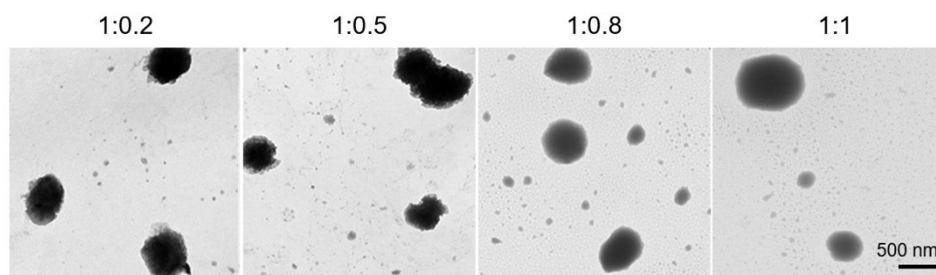


Fig. S2 TEM images of IQ-Cm/DGal aggregates at different molar ratios. [IQ-Cm] = 20 μ M.

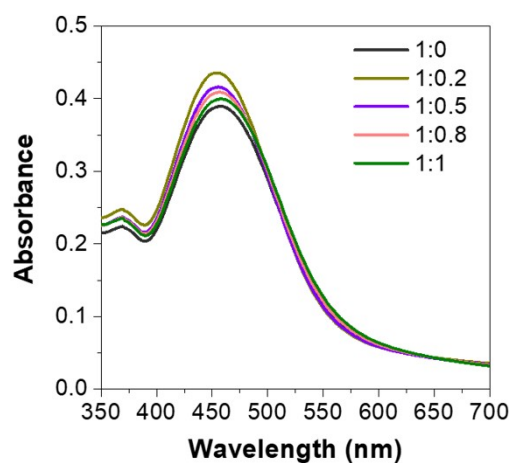


Fig. S3 Absorption spectra of IQ-Cm/DGal aggregates at different molar ratios. [IQ-Cm] = 20 μ M.

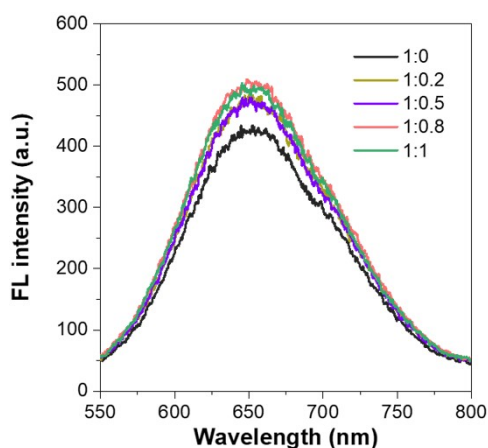


Fig. S4 Fluorescence spectra of IQ-Cm/DGal aggregates at different molar ratios.

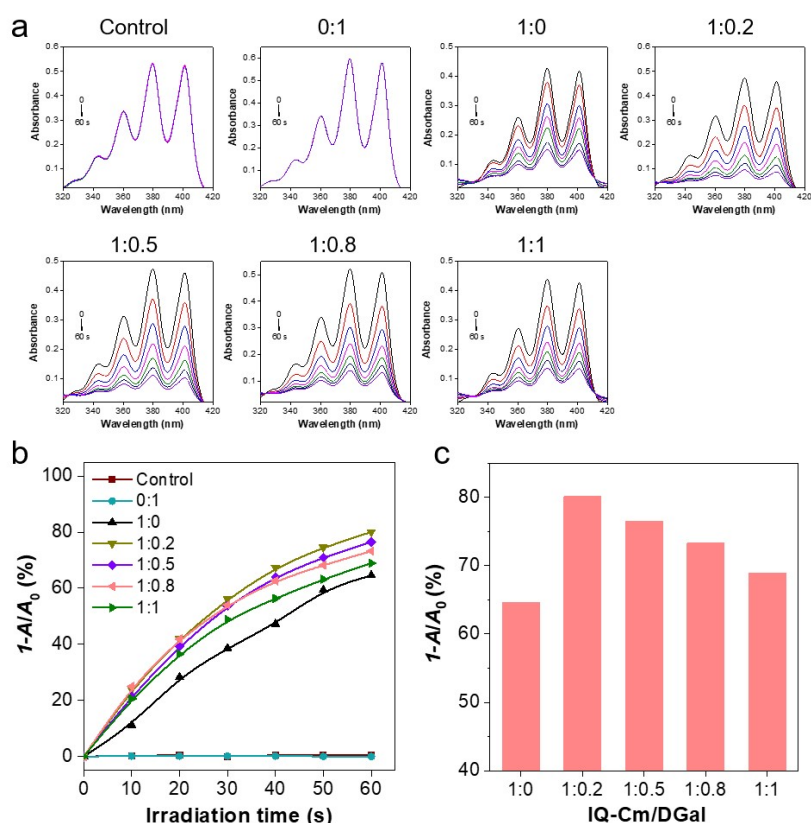


Fig. S5 $^1\text{O}_2$ generation ability of IQ-Cm/DGal aggregates detected by ABDA. (a) Absorption spectra of ABDA ($50\ \mu\text{M}$) without and with IQ-Cm/DGal aggregate of different ratios against the white light irradiation ($20\ \text{mW}/\text{cm}^2$) time. (b) Decomposition rate of ABDA at $379\ \text{nm}$ without and with IQ-Cm/DGal aggregates of different ratios over white light irradiation time ($20\ \text{mW}/\text{cm}^2$) and (c) decomposition rate of ABDA in presence of IQ-Cm/DGal aggregates with different ratios under irradiation for $60\ \text{s}$. $[\text{IQ-Cm}] = 20\ \mu\text{M}$.

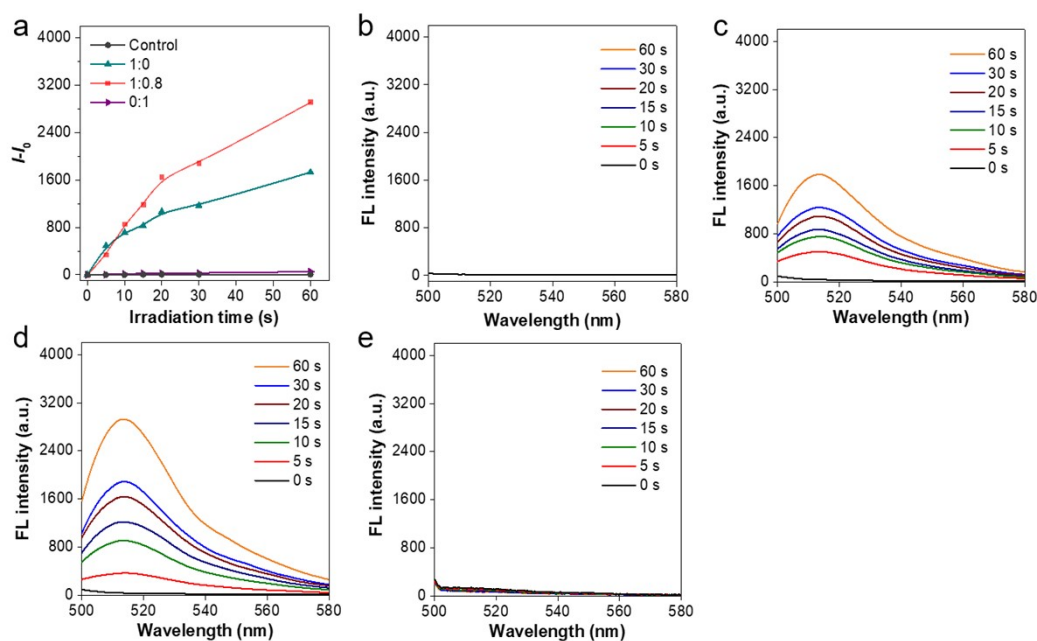


Fig. S6 $\cdot\text{OH}$ generation ability of IQ-Cm/DGal aggregates detected by HPF. (a) Change of fluorescence intensity ($I-I_0$) of HPF at 515 nm without and with the presence of IQ-Cm/DGal aggregates at different ratios against white light irradiation time (20 mW/cm^2). (b)-(e) The fluorescence spectra of HPF ($5 \mu\text{M}$) over white light irradiation time without IQ-Cm/DGal aggregates (b), with IQ-Cm/DGal aggregates at 1:0 (c), 1:0.8 (d) and 0:1 (e), respectively.

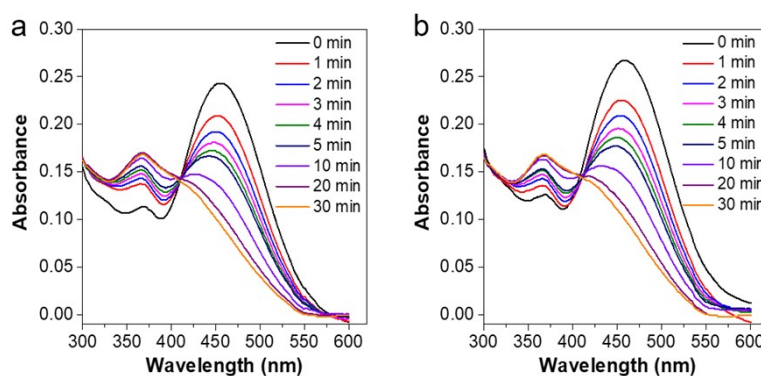


Fig. S7 (a) and (b) Absorbance spectra of IQ-Cm/DGal aggregates at 1:0 and 1:0.8 against light irradiation time (60 mW/cm^2), respectively. $[\text{IQ-Cm}] = 20 \mu\text{M}$.

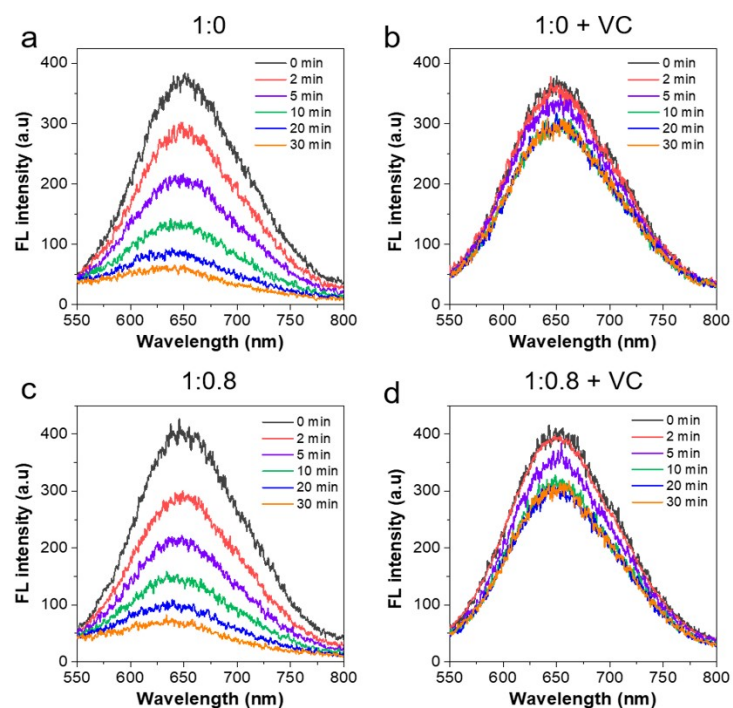


Fig. S8 (a) and (b) Fluorescence spectra of IQ-Cm/DGal aggregates at 1:0 against light irradiation (60 mW/cm^2) time without and with the presence of VC, respectively. (c) and (d) Fluorescence spectra of IQ-Cm/DGal aggregates at 1:0.8 against light irradiation time without and with VC, respectively. $[\text{IQ-Cm}] = 20 \mu\text{M}$ and $[\text{VC}] = 800 \mu\text{M}$.

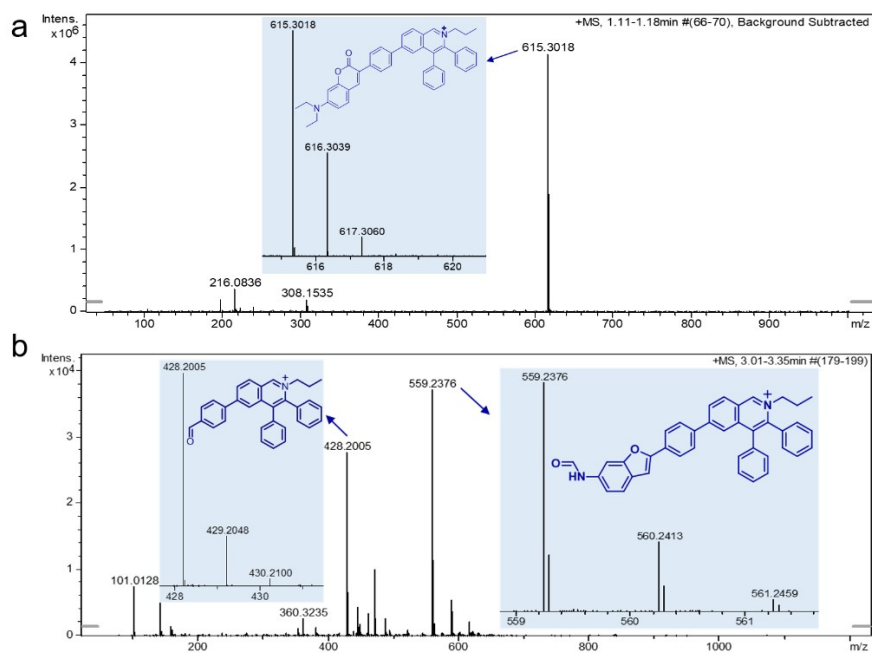


Fig. S9 (a) and (b) HRMS spectra of IQ-Cm before and after L30 in positive ion mode.

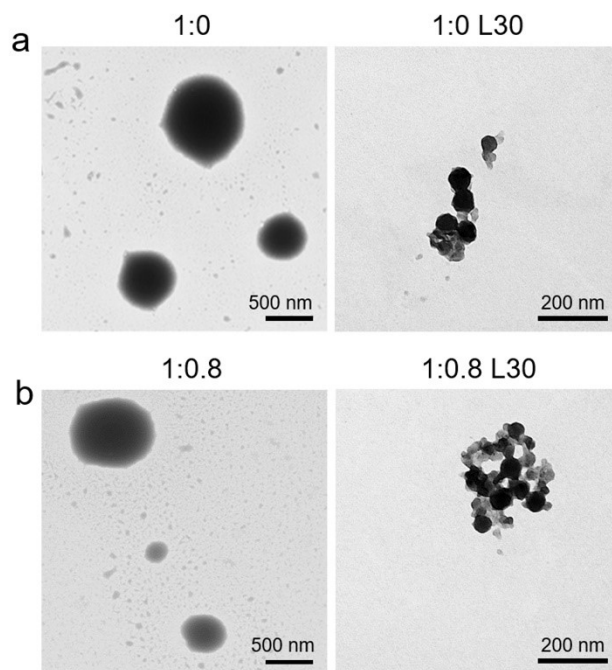


Fig. S10 (a) TEM images of IQ-Cm/DGal aggregates at 1:0 before and after L30. (b) TEM images of IQ-Cm/DGal aggregates at 1:0.8 before and after L30.

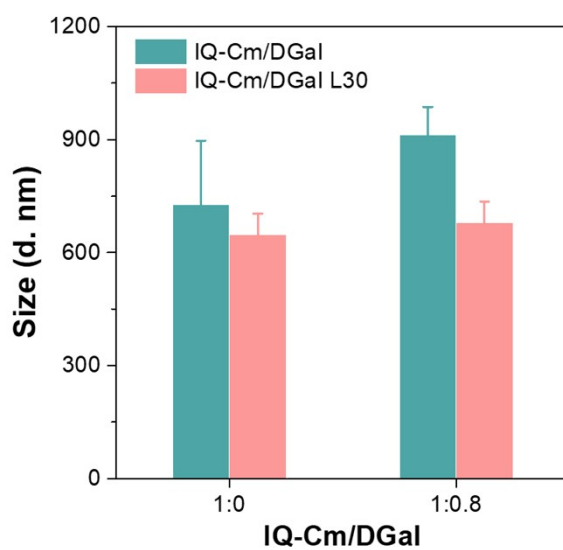


Fig. S11 Size distribution of IQ-Cm/DGal aggregates at 1:0 and 1:0.8 before and after L30. [IQ-Cm] = 20 μ M.

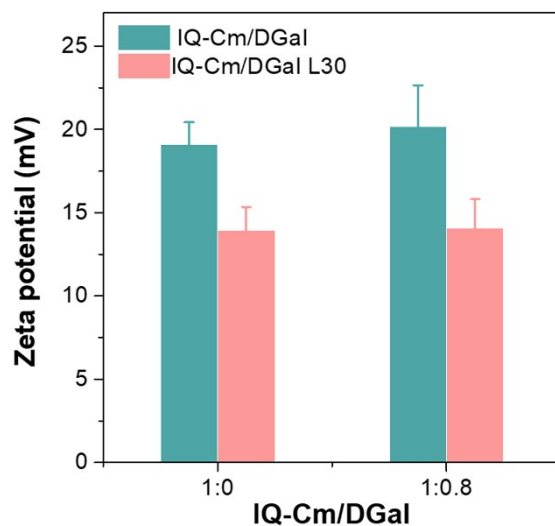


Fig. S12 Zeta potential results of IQ-Cm/DGal aggregates at 1:0 and 1:0.8 before and after L30. [IQ-Cm] = 20 μ M.

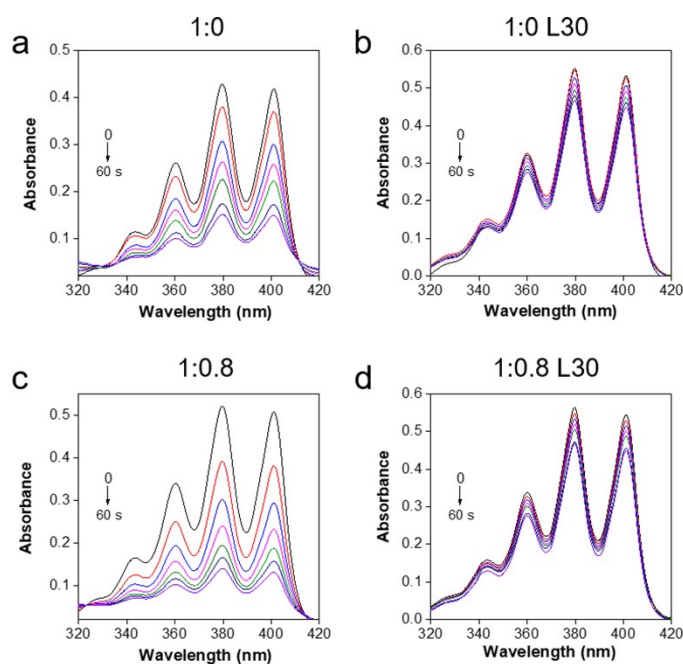


Fig. S13 $^1\text{O}_2$ generation ability of IQ-Cm/DGal aggregates before and after L30. (a-d) The absorption spectra of ABDA against white light (20 mW/cm^2) irradiation time with IQ-Cm/DGal aggregate of 1:0 (a), IQ-Cm/DGal aggregate of 1:0 after L30 (b), IQ-Cm/DGal aggregate of 1:0.8 (c) and IQ-Cm/DGal aggregate of 1:0.8 after L30 (d), respectively.

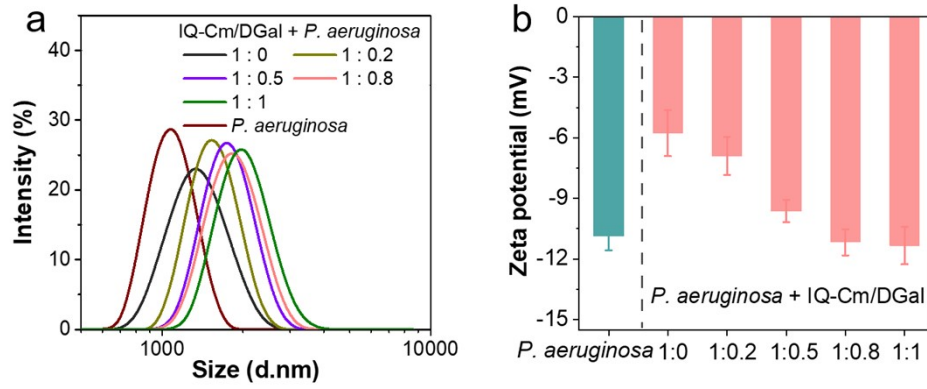


Fig. S14 (a) size distribution and (b) zeta potential results of *P. aeruginosa* before and after incubated with IQ-Cm/DGal aggregates at different ratios for 30 min.

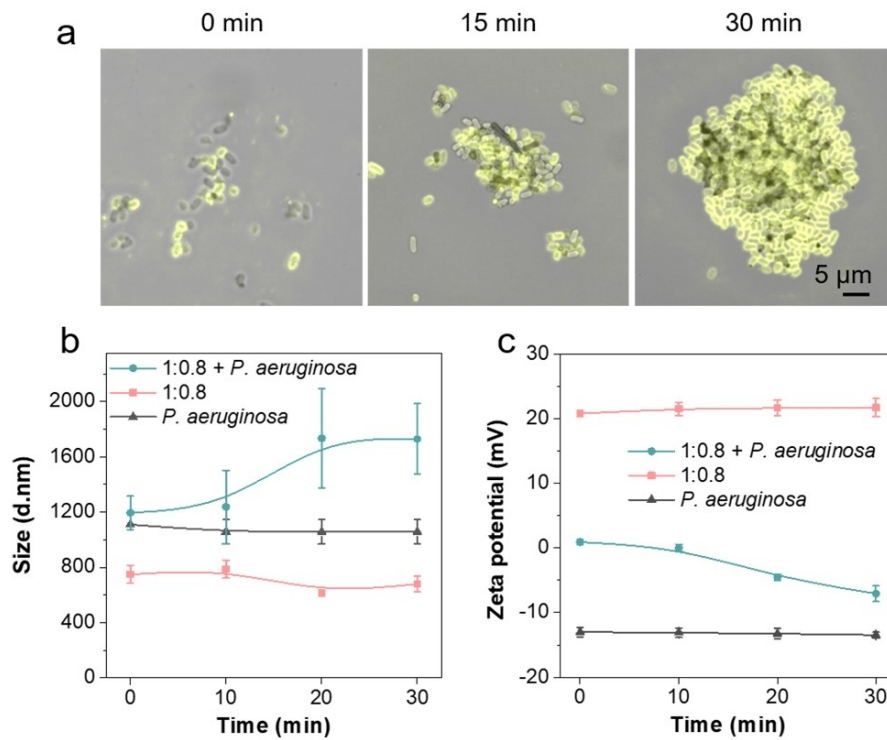


Fig. S15 (a) Merged images of fluorescence and bright field, (b) size distribution and (c) zeta potential results of *P. aeruginosa* after incubated with IQ-Cm/DGal aggregates at 1:0.8 for the different time. [IQ-Cm] = 20 μM.

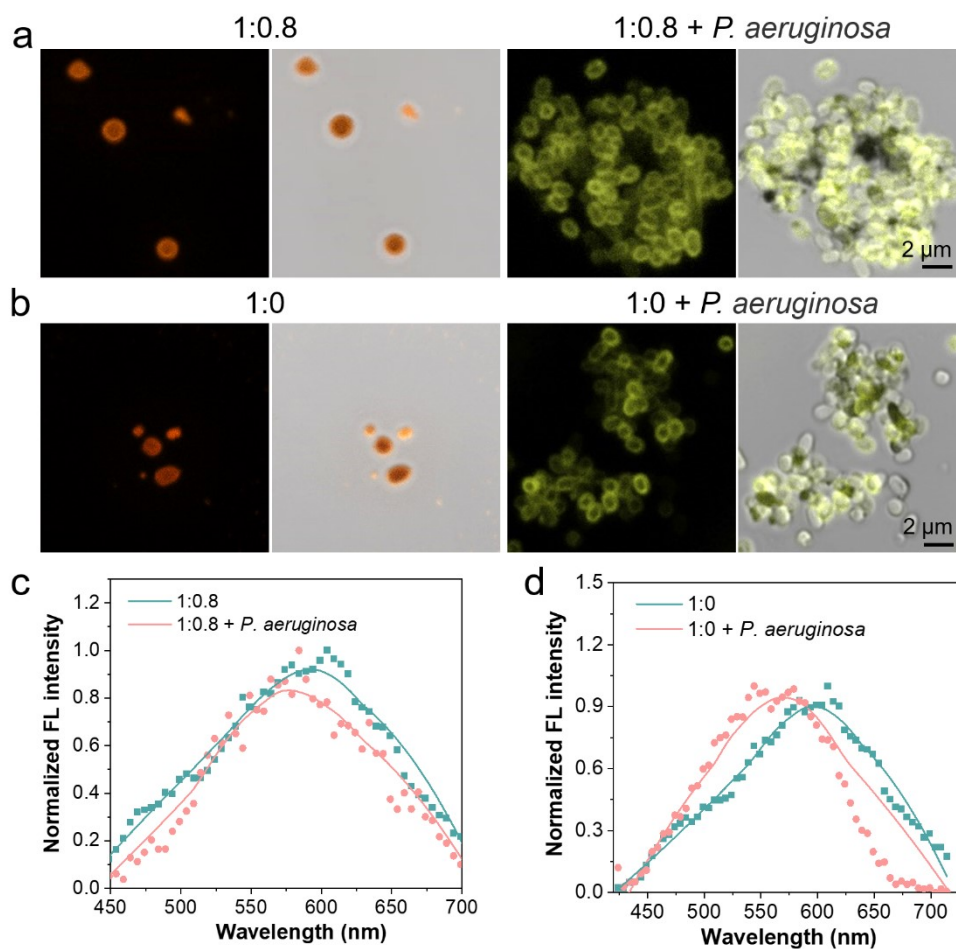


Fig. S16 (a) CLSM images of IQ-Cm/DGal aggregates at 1:0.8 before and after interaction with *P. aeruginosa* for 30 min, respectively. (b) CLSM images of IQ-Cm/DGal aggregates at 1:0 before and after interaction with *P. aeruginosa* for 30 min, respectively. Ex: 405 nm, Em: 420-570 nm. (c) and (d) *In situ* fluorescence spectra of *P. aeruginosa* stained by IQ-Cm/DGal aggregates at 1:0.8 or 1:0 for 30 min and collected under CLSM wavelength scanning mode, respectively. Ex: 405 nm.

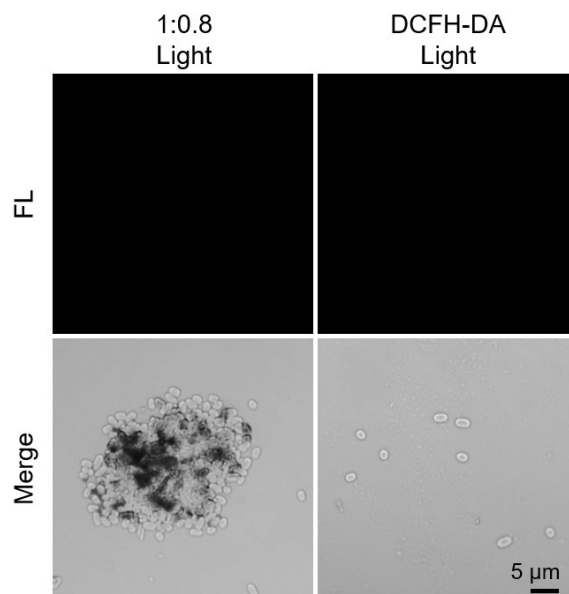


Fig. S17 Fluorescence and merged images of *P. aeruginosa* after incubated with only IQ-Cm/DGal aggregates at 1:0.8 for 10 min or only DCFH-DA (50 μ M) for 20 min, then treated under dark or under white light irradiation for 40 s. Imaging conditions: Ex: 405 nm and Em: 420-570 nm. [IQ-Cm] = 20 μ M.

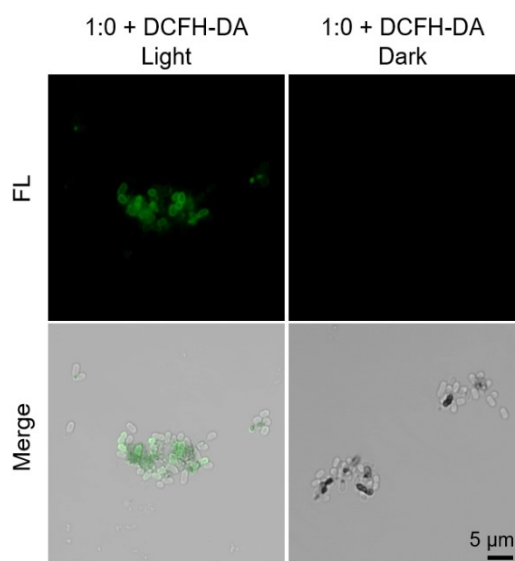


Fig. S18 Fluorescence and merged images of *P. aeruginosa* after incubated with DCFH-DA (50 μ M) for 20 min and IQ-Cm/DGal aggregates (1:0) for 10 min, then treated under dark or under white light irradiation for 40 s. Ex: 405 nm and Em: 420-570 nm. [IQ-Cm] = 20 μ M.

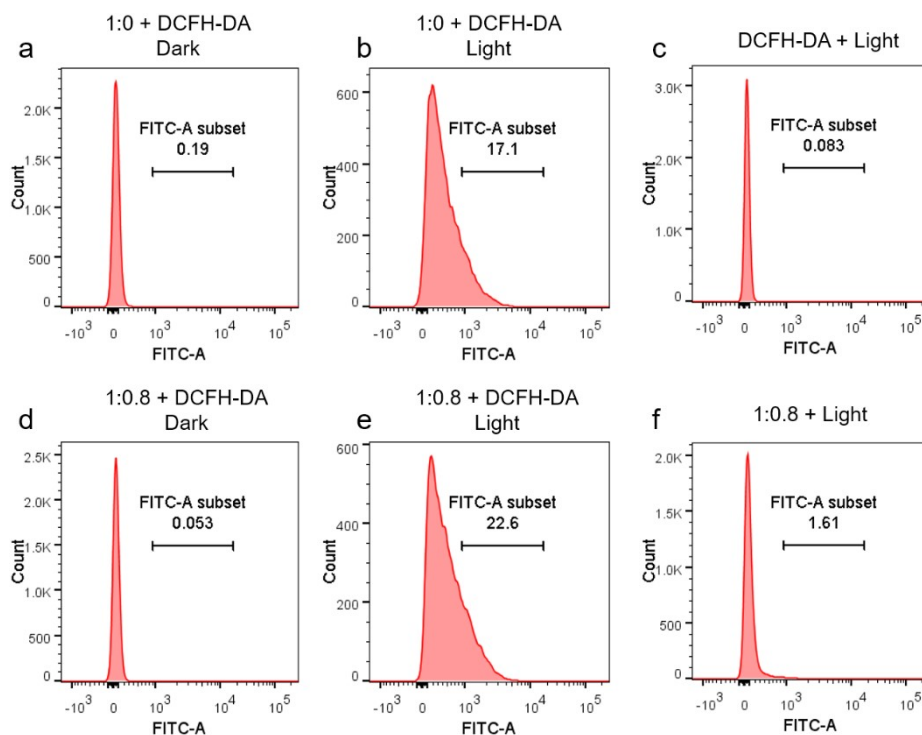


Fig. S19 Flow cytometry analysis of *P. aeruginosa* after treated under different conditions: (a) DCFH-DA and the aggregates (1:0) without light irradiation, (b) DCFH-DA and the aggregates (1:0) with irradiation for 40 s, (c) DCFH-DA with irradiation, (d) DCFH-DA and the aggregates (1:0.8) without irradiation, (e) DCFH-DA and the aggregates (1:0.8) with irradiation and (f) the aggregates (1:0.8) with irradiation.

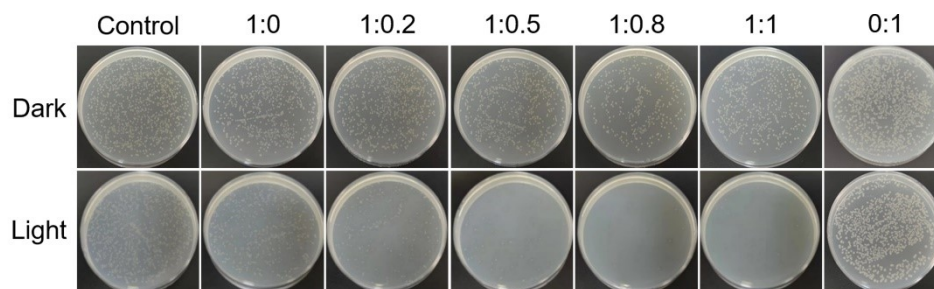


Fig. S20 Photographs of agar plates with the colonies of *P. aeruginosa* before and after treated by IQ-Cm/DGal aggregates with different ratios under darkness or white light irradiation (60 mW/cm^2) for 30 min. $[\text{IQ-Cm}] = 20 \text{ }\mu\text{M}$.

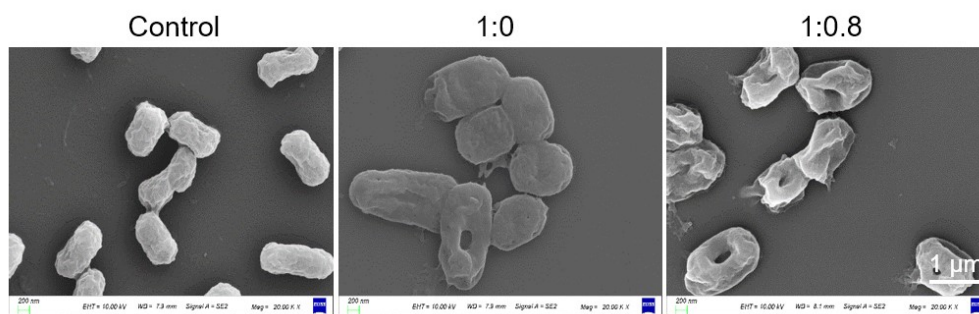


Fig. S21 SEM images of *P. aeruginosa* before (control) and after treated by the IQ-Cm/DGal aggregates (1:0 or 1:0.8) under light irradiation (60 mW/cm², 30 min). [IQ-Cm] = 20 μM.

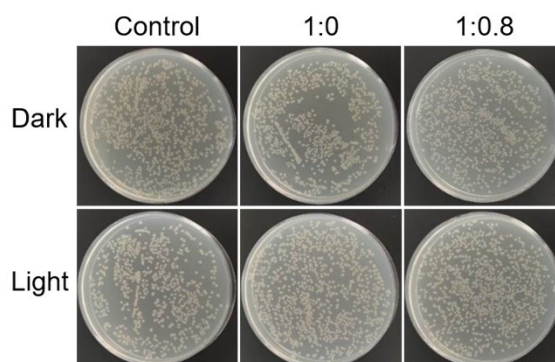


Fig. S22 Photographs of agar plates with *P. aeruginosa* colonies without and with incubated by IQ-Cm/DGal aggregates (1:0 or 1:0.8) after L30 under darkness or white light irradiation (60 mW/cm²) for 30 min. [IQ-Cm] = 20 μM.

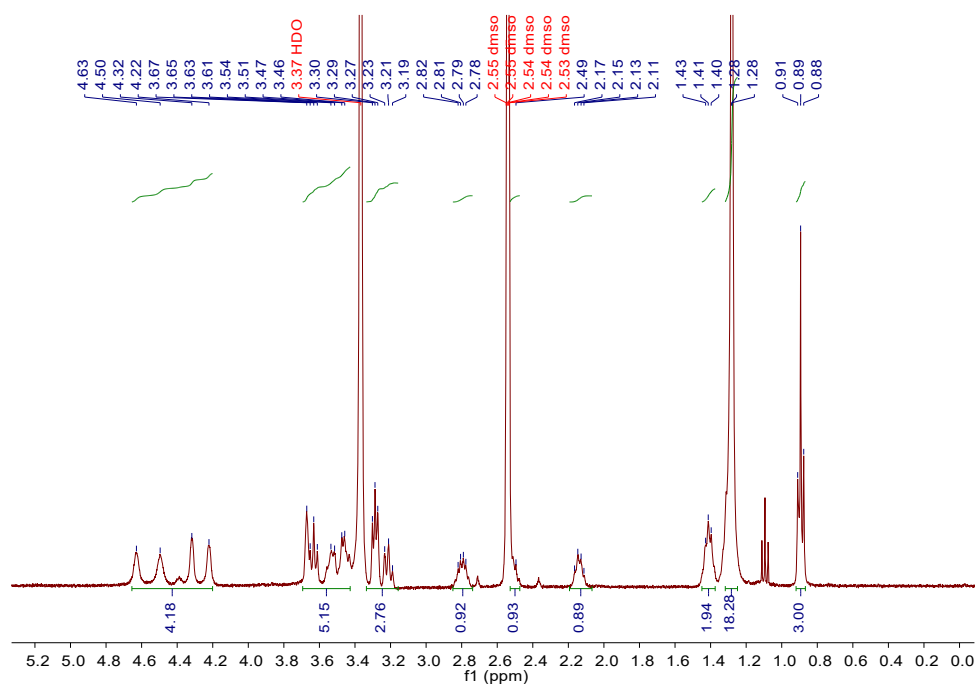


Fig. S23 ¹H NMR spectrum of DGal in DMSO-*d*₆.

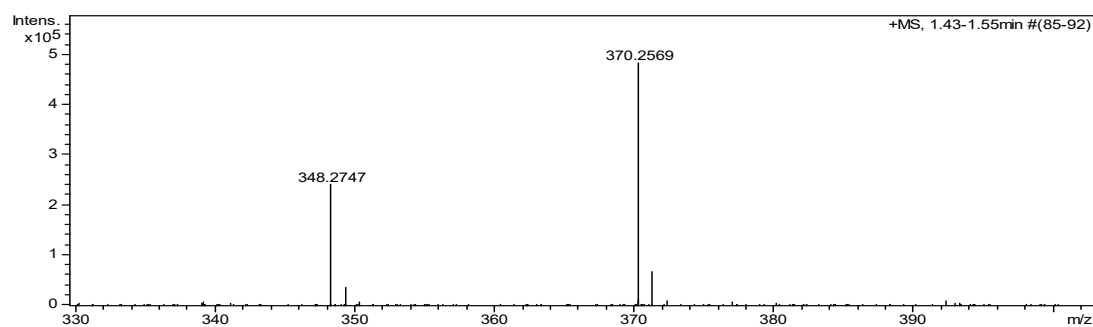


Fig. S24 HRMS spectrum of DGal in positive ion mode.

References

- 1 a) C. Zhou, M. Jiang, J. Du, H. Bai, G. Shan, R. T. K. Kwok, J. H. C. Chau, J. Zhang, J. W. Y. Lam, P. Huang, B. Z. Tang, *Chem. Sci.* 2020, **11**, 4730-4740; b) V. Neto, A. Voisin, V. Héroguez, S. Grelier, V. Coma, *J. Agric. Food Chem.* 2012, **60**, 10516-10522.
- 2 Q. Guo, S. Xue, J. Feng, C. Peng, C. Zhou, Y. Qiao, *Adv. Healthcare Mater.* 2023, **12**, 2300818.